PHYSICAL REVIEW B VOLUME 32, NUMBER 6 15 SEPTEMBER 1985

Brownian motion and vibrational phase relaxation at surfaces: CO on Ni(111)

B. N. J. Persson
Institut für Festkörperforschung der Kernforschungsanlage Jülich, D-5170 Jülich, West Germany

R. Ryberg
Department of Physics, Chalmers University of Technology, S-412 96 Gothenburg, Sweden

(Received 11 January 1985)

The temperature dependence of the internal stretch vibrational mode of CO chemisorbed on Ni(111) has been studied with the use of infrared spectroscopy. The width of the absorption peak of the bridge-bonded molecules exhibits a strong temperature dependence. A theory is developed which accounts well for the experimental results. It shows that the peak broadening is caused by anharmonic coupling to one particular low-frequency mode, namely a hindered rotation.

I. INTRODUCTION

Much work has been done in recent years towards a better understanding of what determines the linewidth and line shape of vibrational modes in solids, in liquids, and at surfaces. Such studies can give important information about the processes that give rise to vibrational energy relaxation and redistribution,[1-4] as discussed in particular by Marks *et al.*[2]

The absorption spectrum as obtained using infrared spectroscopy or Raman scattering can be written as

$$I(\omega)\sim\int_{-\infty}^{\infty}dt\,e^{i\omega t}\langle u(t)u(0)\rangle\ , \tag{1}$$

where $u(t)$ is the relevant normal mode coordinate and where $\langle\ \rangle$ stands for a thermal average. Equation (1) is a suitable starting point for a discussion of vibrational line shapes. For example, if

$$\langle u(t)u(0)\rangle\sim e^{-i\Omega t-|t|/\tau}\ ,$$

then

$$I(\omega)\sim\int_{-\infty}^{\infty}dt\,e^{i(\omega-\Omega)t-|t|/\tau}=\frac{-2/\tau}{(\Omega-\omega)^2+1/\tau^2}\ ,$$

i.e., $I(\omega)$ is a Lorentzian centered at $\omega=\Omega$ and with a full width at half maximum (FWHM) of $2/\tau$. Now there are two different ways in which the correlation function $\langle u(t)u(0)\rangle$ can decay with increasing time:

(a) *Vibrational energy relaxation:* After the excitation, the oscillator amplitude $u(t)$ decays. This can be caused by emission of phonons or, for adsorbates on a metal surface, by excitation of electron-hole pairs.

(b) *Vibrational phase relaxation:* The amplitude of $u(t)$ is constant but the definite phase relation that exists between $u(t)$ and $u(0)$ for a free oscillator $[u(t)=u(0)\exp(-i\Omega t)]$ is destroyed because of elastic scattering with thermally excited phonons (or electron-hole pairs). That this leads to a decay of the correlation function $\langle u(t)u(0)\rangle$ is seen if we consider an ensemble of N oscillators. If they all are excited in phase at time $t=0$, they will, in general, have different phases at time $t>0$ caused by this interaction. Thus, the correlation function $\langle u(t)u(0)\rangle$, which can be considered as an ensemble average, will decay towards zero as $t\rightarrow\infty$.

From (1) it follows that

$$\int d\omega\,I(\omega)\sim\langle u^2(0)\rangle\sim\coth(\beta\Omega/2)\ ,$$

where $\beta=1/k_BT$ (T is the temperature and k_B the Boltzmann constant). In the present work, we will only consider the line shape of high-frequency modes, giving $\beta\Omega\gg1$ for all temperatures of interest. Thus $\coth(\beta\Omega/2)\approx1$ and the area under the line profile $I(\omega)$ is practically temperature independent. The interaction between the high-frequency mode Ω and the surrounding will shift and broaden the absorption peak but not change the integrated absorbtance (as long as the interaction is "weak").

In general, the relative importance between vibrational energy and phase relaxation at metal surfaces is quite different from that in (nonmetallic) solids and liquids or at nonmetallic surfaces. The reason is that in the latter case energy relaxation of a high-frequency (Ω) mode can only occur via multiphonon emission (which has a very small probability if $\Omega\gg\omega_{\max}$, where $\omega_{\max}$ is the highest phonon frequency of the surrounding media). For adsorbates on a metal surface, the additional decay path caused by electron-hole pair excitation exists[5] and is particularly important for high-frequency modes since the phase-space for electron-hole pair excitation is proportional to Ω. On the other hand, on nonmetallic surfaces (e.g., undoped semiconductor surfaces) one would expect vibrational phase relaxation to dominate for all high-frequency modes by many orders of magnitude (in solids and liquids cases are known where phase relaxation is more than 10 orders of magnitude faster than energy relaxation; such as the N—N stretch vibration in liquid nitrogen[6]).

Several experimental line-shape studies of vibrational modes of molecules adsorbed on metal surfaces have been published.[7-12] In a very recent letter,[13] we have shown that the C—O stretch vibration of CO on a Cu(100) surface has a temperature-independent Lorentzian line shape with a width (FWMH) of 4.5 cm^{-1}. This linewidth is caused by vibrational energy relaxation, via excitations of electron-hole pairs. Decay via phonon emission would require that at least 8 phonons are emitted, which has a very small probability. On the other hand, for low-frequency modes such as the Ni-CO vibration on Ni(100) decay via two-phonon emission is energetically possible and probably the relevant energy relaxation process. Chiang *et al.*[11] found at room temperature a linewidth of 15 cm^{-1} for the Ni-CO vibrational mode, which agrees well with theoretical predictions.[14,15]

Recently, Hayden and Bradshaw[10] have reported a strong temperature dependence of the line shapes for the C—O stretch vibrational mode on Pt(111). Similarly, Trenary *et al.*[12] found a strong temperature dependence in the linewidth for CO on Ni(111). This temperature dependence cannot be due to multiphonon emission which has negligible probability. Furthermore, damping via electron-hole pair excitation is practically temperature independent.[16] Thus, it is likely that the temperature dependence of these vibrational lines is caused by vibrational phase relaxation.[4,12] In this work we will discuss this problem in more detail and present a combined experimental-theoretical study which clearly reveals the nature of the phase relaxation process.

II. BROWNIAN MOTION MODEL

We consider the following problem: A diatomic molecule *AB* is adsorbed on a metal surface. The frequency Ω of the internal *A—B* stretch vibrational mode depends on the bonding position on the surface (for CO, Ω increases typically with about 10% when going from bridge to on-top position). This variation in the internal vibrational frequency with bonding position will, at temperatures where the molecules are mobile, lead to a broadening of the vibrational line.

Due to the screening by the substrate conduction electrons, Ω will depend only on the position of a small number of neighboring lattice atoms. We call these atoms together with the *AB* molecule for the cluster. The normal mode frequencies of the cluster are denoted by $\bar{\omega}_\mu$ and the corresponding coordinates by Q_μ. Of the vibrational modes involving the *AB* molecule one distinguishes (somewhat loosely) between frustrated translations and frustrated rotations. The former involves mainly translational (but also some rotational) and the latter mainly rotational (but also some translational) motion of the *AB* molecule.

Assume now that the *A—B* stretch vibration frequency Ω depends mainly on *one* of the other normal mode coordinates Q (frequency $\bar{\omega}_0$), so that $\Omega \approx \Omega(Q)$. For example (as will be shown later), for CO in bridge position on Ni(111) the dominating coupling is to a frustrated rotation. Assume also that the system is symmetric as $Q \to -Q$. As low enough temperatures, where $\langle Q^2 \rangle$ is small, we can expand

$$\Omega^2(Q) \approx \Omega_0^2 + a\Omega_0 Q^2 , \tag{2}$$

where a is a constant. If $u(t)$ denotes the normal mode coordinate for the *A—B* stretch vibration, then the equation of motion for this coordinate becomes

$$m^* \ddot{u} + m^* \Omega_0^2 u + m^* a \Omega_0 Q^2 u = 0 . \tag{3}$$

Under some assumptions, which are discussed in Appendix A, the equation of motion for the coordinate Q is

$$m\ddot{Q} + m\omega_0^2 Q + m\eta\dot{Q} + m^* a\Omega_0 u^2 Q = f(t) . \tag{4}$$

In this equation we have now accounted for the coupling between the cluster and the rest of the crystal, which has three effects[17–19] (see Appendixes A and B): It renormalizes the cluster frequency ($\bar{\omega}_0 \to \omega_0$). It introduces a friction force which we simply take to be of the Markoff form $m\eta\dot{Q}$. The physical origin of the friction force is that the Q motion is damped due to excitations of phonons and electron-hole pairs. Finally, it introduces a fluctuating force, which in accordance to the fluctuation-dissipation theorem satisfies

$$\langle f(t) f(0) \rangle = 2\eta m k_B T \delta(t) . \tag{5}$$

The solution of the system of equations (3)—(5) represents a complicated mathematical problem but we have recently[20] presented a quite general solution, which is valid beyond the Markoff approximation, i.e., with a frequency-dependent friction in the equation of motion (4) for the Q coordinate. Here we will only discuss a simple limiting case which clearly exhibits the basic physics involved and which defines the relevant physical quantities.

Assume that the fourth term in (4) can be neglected compared with the third term—this is obviously possible only if

$$m^* \,|\, a \,|\, \Omega_0 u^2 \ll m\eta\omega_0 .$$

In the first vibrational excited state we have $u \sim (\hbar/2m^*\Omega_0)^{1/2}$; thus the inequality above takes the form

$$\hbar \,|\, a \,|\, /2 \ll m\eta\omega_0$$

or

$$|\, \delta\omega \,| \ll \eta , \tag{6}$$

where

$$\delta\omega = \hbar a / 2m\omega_0 = a Q_0^2 , \tag{7}$$

where $Q_0 = (\hbar/2m\omega_0)^{1/2}$ is a displacement characteristic of the zero-point motion.

The quantities $\delta\omega$ and η and the resonance frequency ω_0 are the basic parameters which enter in the phase relaxation process. In Appendix B and Sec. III we discuss the friction parameter η. Here we present a simple discussion of $\delta\omega$. Assume first that Q corresponds to a frustrated translation. For a rough estimate we take

$$\Omega(Q) \approx \Omega_0 + \tfrac{1}{2}\Delta\Omega[1 - \cos(2\pi Q/d)]$$
$$\approx \Omega_0 + \Delta\Omega(2\pi Q/d)^2/4 ,$$

where d is the surface lattice constant. We get $a = \Delta\Omega 2\pi^2/d^2$ and

$$\delta\omega = 2\pi^2 \Delta\Omega (Q_0/d)^2 . \tag{8}$$

For CO, $m = 28$ u and if $\omega_0 \sim 100$ cm^{-1}, then $Q_0 \approx 0.1$ Å. With $d = 3$ Å and $\Delta\Omega \sim 100$ cm^{-1} one gets $\delta\omega \approx 2$ cm^{-1}. For most metals (see Appendix B and Sec. III), $\eta \sim 30$ cm^{-1} when $\omega_0 \sim 100$ cm^{-1}. Thus, in this case, the inequality $|\delta\omega| \ll \eta$ is well satisfied. Physically, this means that the response back on the Q motion from the high-frequency vibration is negligible compared with the damping force $m\eta\dot{Q}$.

Let us now consider a frustrated rotation. Q is now an angle variable and for a rough estimate we take

$$\Omega(Q) \approx \Omega_0 + \tfrac{1}{2}\Delta\Omega(1-\cos Q)$$
$$\approx \Omega_0 + \Delta\Omega\, Q^2/4 \ .$$

Thus $a \approx \Delta\Omega/2$ and

$$\delta\omega = \Delta\Omega\, Q_0^2/2 \ , \tag{9}$$

where $Q_0 = (\hbar/2I\omega_0)^{1/2}$ is a tilting angle characteristic of the zero-point motion. With $\omega_0 \sim 100\ \text{cm}^{-1}$ and $I = ml^2 \sim 16u \times (1\ \text{Å}^2)$ we get $Q_0 \approx 0.2 \simeq 10°$. Thus if $\Delta\Omega \sim 100\ \text{cm}^{-1}$ then $\delta\omega \approx 2\ \text{cm}^{-1}$.

If $\delta\omega$ always was this small for frustrated translations and rotations, then practically no observable contribution to the linewidth and frequency shift would result [using Eqs. (22) and (23) below with $\eta = 30\ \text{cm}^{-1}$, $\delta\omega = 2\ \text{cm}^{-1}$, and $\omega_0 = 100\ \text{cm}^{-1}$ gives at room temperature a frequency shift $\Delta\omega \sim 4\ \text{cm}^{-1}$ and a linewidth $\gamma = 1\ \text{cm}^{-1}$].

Equations (3) and (4) can now be written as

$$\ddot{u} + (\Omega_0^2 + a\Omega_0 Q^2)u = 0 \ , \tag{10}$$

$$\ddot{Q} + \eta\dot{Q} + \omega_0^2 Q = f/m \ . \tag{11}$$

Our basic problem is now to calculate the line-shape function

$$I(\omega) = \int dt\, e^{i\omega t}\langle u(t)u(0)\rangle \tag{12}$$

from Eqs. (10) and (11). This can be done as follows: First, we rewrite (10) as

$$\ddot{u} + [\Omega_0^2 + \Omega_0 A(t)]u = 0 \ , \tag{13}$$

where

$$A(t) = aQ^2 \ .$$

Next, we write

$$u = \alpha(t)e^{i\Omega_0 t} + \text{H.c.}$$

and substitute this in (13),

$$\ddot{\alpha} + 2i\Omega_0\dot{\alpha} - \Omega_0^2\alpha + [\Omega_0^2 + \Omega_0 A(t)]\alpha = 0$$

or

$$2i\Omega_0\dot{\alpha} + \Omega_0 A\alpha = 0 \ ,$$

where we have neglected the $\ddot{\alpha}$ term which is small when $|A| \ll \Omega_0$. Thus we get

$$\alpha(t) = \alpha(0)\exp\left[\frac{i}{2}\int_0^t dt'\, A(t')\right]$$

and

$$u(t) = \alpha(0)\exp\left[\frac{i}{2}\int_0^t dt'\, A(t') + i\Omega_0 t\right] + \text{H.c.}$$

Substituting this in (12) gives

$$I(\omega) \propto \int dt\, e^{i\omega t}\left[e^{i\Omega_0 t}\left\langle \exp\left[\frac{i}{2}\int_0^t dt' A(t')\right]\right\rangle + \text{c.c.}\right] . \tag{14}$$

Next, we use the cumulant expansion[21] to second order in A

$$\left\langle \exp\left[\frac{i}{2}\int_0^t dt' A(t')\right]\right\rangle = e^{i\langle A\rangle t/2 - H(t)} \ , \tag{15}$$

where

$$H(t) = \tfrac{1}{4}\int_0^t dt' \int_0^{t'} dt''\, h(t'-t'') \ , \tag{16}$$

$$h(t) = \langle A(t)A(0)\rangle - \langle A(0)\rangle^2 \ . \tag{17}$$

We now calculate $\langle A\rangle$ and $h(t)$ using the equation of motion (11). We get

$$\langle A\rangle = a\langle Q^2\rangle = ak_B T/m\omega_0^2 \ .$$

Furthermore, since f is a Gaussian random variable,

$$\langle Q^2(t)Q^2(0)\rangle = \langle Q^2(0)\rangle^2 + 2\langle Q(t)Q(0)\rangle^2 \ ,$$

so that

$$h(t) = \langle A(t)A(0)\rangle - \langle A(0)\rangle^2 = 2a^2\langle Q(t)Q(0)\rangle^2 \ . \tag{18}$$

Now $\langle Q(t)Q(0)\rangle$ is easily calculated from (11):

$$\langle Q(t)Q(0)\rangle = \frac{1}{\omega_2-\omega_1}(\omega_2 e^{\omega_1 t} - \omega_1 e^{\omega_2 t})\langle Q^2\rangle^2 \ , \tag{19}$$

where

$$\omega_{1,2} = -\frac{\eta}{2} \pm i(\omega_0^2 - \eta^2/4)^{1/2} \ .$$

Substituting (19) in (18) gives

$$h(t) = \frac{-4a^2}{(\omega_2-\omega_1)^2}\omega_1\omega_2 e^{(\omega_1+\omega_2)t}\langle Q^2\rangle^2 \ , \tag{20}$$

where we have neglected the terms $\sim e^{2\omega_1 t}$ and $\sim e^{2\omega_2 t}$, which both oscillate rapidly in time and give no contribution to the linewidth or shift. (These two terms give rise to absorption peaks at $\Omega \pm 2\omega_0$ corresponding to the emission or absorption of two vibrational quanta ω_0 together with the internal A-B vibrational mode Ω.) Substituting the explicit expressions for ω_1 and ω_2 in (20) and assuming that $\omega_0^2 \gg \eta^2/4$ we get

$$h(t) = a^2 e^{-\eta t}\langle Q^2\rangle^2 \ ,$$

and thus

$$H(t) = \frac{a^2\langle Q^2\rangle^2}{4\eta^2}(\eta t + e^{-\eta t} - 1) \equiv H_0(\eta t + e^{-\eta t} - 1) \ .$$

Combining this result with (14) and (15) gives

$$I(\omega)= \int dt\, e^{i\omega t}\{ \exp[-i(\Omega_0+\tfrac{1}{2}\langle A\rangle)t-H_0(\eta\,|t|+e^{-\eta|t|}-1)]+\text{c.c.}\}$$
$$\approx e^{H_0}\sum_{n=0}^{\infty}(-H_0)^n\frac{1}{n!}\frac{2\eta(H_0+n)}{(\omega-\Omega_0-\frac{1}{2}\langle A\rangle)^2+[\eta(H_0+n)]^2}\,, \tag{21}$$

where we have neglected the nonresonant (for $\omega>0$) term. For $|H_0|\ll 1$, Eq. (21) reduces to

$$I(\omega)\approx\frac{2H_0\eta}{(\omega-\Omega_0-\frac{1}{2}\langle A\rangle)^2+(H_0\eta)^2}\,.$$

Thus, in this limit, the line shape is a Lorentzian with the center frequency

$$\omega=\Omega_0+\tfrac{1}{2}\langle A\rangle=\Omega_0+\tfrac{1}{2}a\langle Q^2\rangle$$

and the linewidth (FWHM)

$$\gamma=2H_0\eta=\frac{a^2}{2\eta}\langle Q^2\rangle^2\,.$$

With the definition (7), we can write the (temperature-dependent) frequency shift as

$$\Delta\omega=\tfrac{1}{2}\,\delta\omega\frac{\langle Q^2\rangle}{Q_0^2}=\frac{k_BT}{\omega_0}\delta\omega \tag{22}$$

and the linewidth as

$$\gamma=\frac{1}{2\eta}\left[\delta\omega\frac{\langle Q^2\rangle}{Q_0^2}\right]^2=\left[\frac{k_BT}{\omega_0}\right]^2\frac{2(\delta\omega)^2}{\eta}\,, \tag{23}$$

where

$$Q_0=(\hbar/2m\omega_0)^{1/2} \tag{24}$$

is the amplitude of the zero-point motion. In deriving the equations above, we have assumed that the temperature T is so high that we are in the Boltzmann-statistic regime. However, the expressions for $\Delta\omega$ and γ are probably valid for all temperatures if we calculate $\langle Q^2\rangle$ quantum mechanically and subtract away the zero-point contribution:

$$\Delta\omega=\frac{\delta\omega}{e^{\beta\omega_0}-1}\,, \tag{25}$$

$$\gamma=\frac{e^{\beta\omega_0}}{(e^{\beta\omega_0}-1)^2}\frac{2(\delta\omega)^2}{\eta}\,. \tag{26}$$

We note that $\Delta\omega$ and $\gamma\sim e^{-\beta\omega_0}$ as $T\to 0$ which indeed is the correct low-temperature dependence of these quantities, as shown by Harris *et al.*[22] These authors have shown that the line profile $I(\omega)$ at low temperature, independent of the relative magnitude of $\delta\omega$ and η, has a Lorentzian shape with frequency shift and width given by[21,22]

$$\Delta\omega=e^{-\beta\omega_0}\delta\omega\frac{\eta^2}{(\delta\omega)^2+\eta^2} \tag{27}$$

and

$$\gamma=2e^{-\beta\omega_0}\eta\frac{(\delta\omega)^2}{(\delta\omega)^2+\eta^2}\,. \tag{28}$$

In the general case where $\delta\omega$, η, and T are arbitrary, it is not possible to derive any simple expression for $\Delta\omega$ and γ. Here the line shape $I(\omega)$ is approximately given by[20,22,23]

$$I(\omega)\sim \operatorname{Im}D(\omega)\,, \tag{29}$$

where $(n,m=0,1,\dots,L)$

$$D(\omega)=\sum_{n,m}D_{nm}(\omega)\,. \tag{30}$$

The matrix D_{nm} satisfies the equation

$$\overleftrightarrow{\mathrm{D}}=\overleftrightarrow{\mathrm{P}}\cdot(\omega\overleftrightarrow{\mathbb{1}}-\overleftrightarrow{\mathrm{h}}-\overleftrightarrow{\mathrm{M}})^{-1}\,, \tag{31}$$

where

$$P_{nm}=\delta_{nm}e^{-n\beta\omega_0}(1-e^{-\beta\omega_0})\,,$$
$$h_{nm}=\delta_{nm}(\Omega_0+n\delta\omega)\,, \tag{32}$$

$$M_{nm}=-\delta_{nm}i\eta(2nn_b+n+n_b)+\delta_{n,m+1}i\eta n(n_b+1)$$
$$+\delta_{n,m-1}i\eta m n_b\,, \tag{33}$$

except for $n=m=L$ where

$$M_{LL}=-i\eta L(n_b+1)\,. \tag{34}$$

In the expressions above

$$n_b=[\exp(\beta\omega_0)-1]^{-1}$$

is the Bose-Einstein factor. The dimension $L+1$ of the matrices must be chosen so large that the result is converged, i.e., unchanged if L is increased further. Equations (29)—(34) have been derived within the Markoff approximation but we have recently generalized this result beyond this approximation.[20] The formulas (29)—(34) reduce to (25) and (26) for $\eta/\delta\omega\gg 1$ (or, more exactly, for $\eta/\delta\omega\, n_b\gg 1$) and to (27) and (28) as $T\to 0$. The latter result has been shown by Harris *et al.*[21] by limiting the dimension of the matrices to two (which is a good approximation at low temperatures) and inverting the matrix $(\omega\overleftrightarrow{\mathbb{1}}-\overleftrightarrow{\mathrm{h}}-\overleftrightarrow{\mathrm{M}})$ analytically. The theoretical results presented in Sec. V are calculated from Eqs. (29)—(34) by inverting $(\omega\overleftrightarrow{\mathbb{1}}-\overleftrightarrow{\mathrm{h}}-\overleftrightarrow{\mathrm{M}})$ numerically.

III. FRICTION PARAMETER η

In this section we will discuss the damping of frustrated translations at surfaces. These results are interesting on their own but can also be used as basis for rough *estimates* of the friction coefficient η entering the equation of motion (4) for the coordinate Q.

Let x denote the position of a molecule on a surface and let $V(x)$ be the ground-state potential-energy surface. Since $V(x)$ must have the same periodicity as the underlying surface crystal structure it can be written as a sum over reciprocal-lattice vectors. For simplicity, assume that

$$V(x) = -E_0 - V_0\cos(g_0 x)\ ,$$

where $g_0 = 2\pi/a$ and a is the surface lattice constant. Within this approximation, $2V_0$ is the activation energy for diffusion along the surface which is known for many molecule-metal systems. For low-amplitude vibrations around $x=0$ we can expand

$$V(x) \approx -(E_0+V_0)+\tfrac{1}{2}V_0 g_0^2 x^2 \equiv -(E_0+V_0)+\tfrac{1}{2}m\bar{\omega}_0^2 x^2\ , \tag{35}$$

where m is the mass of the molecule. Thus

$$\hbar\bar{\omega}_0 \simeq (\hbar^2 V_0 g_0^2/m)^{1/2} = 0.39(V_0/ma^2)^{1/2}\ ,$$

with $\hbar\omega_0$ and V_0 in eV, m in u, and a in Å. For CO adsorbed on close-packed metal surfaces [e.g., the (111) surfaces on fcc crystals] the corrugation $2V_0$ in the ground-state chemisorption potential $V(x)$ is very small, typically $2V_0 \sim 0.2$ eV. With $m=28$ u and $a \sim 2$ Å, one gets $\hbar\bar{\omega}_0 = 10$ meV. The highest phonon frequency of many metals (e.g., Ni) is about 30 meV, so that the activation energy of the frustrated translation is well down in the bulk phonon band. Thus this vibration is not a localized mode, but rather a resonance with a width determined by the rate of one-phonon emission. In this section, we will estimate the damping of frustrated translations caused by bulk and surface phonon emission.

We assume that $\omega_0 \ll \omega_{\max}$, where $\omega_{\max}$ is the highest phonon frequency of the crystal. Thus the damping of the frustrated translation x will involve emission of relatively long wavelength phonons and we will be in the linear region of the metal phonon dispersion relation. Thus we can, as a first approximation, use the elastic continuum model to calculate the damping of the frustrated translation x. It is shown in Appendix B that the friction force acting on the x motion from phonon emission can be written as

$$F_{\parallel} = -m\eta_{\parallel}\dot{x}\ ,$$

where

$$\eta_{\parallel} = \frac{1}{8\pi}\frac{m}{\rho}\left[\frac{\omega_0}{c_T}\right]^3 \xi_{\parallel}\omega_0 \tag{36}$$

and

$$\xi_{\parallel} = \mathrm{Re}\left[\int_0^{\infty} dx \left[\frac{1}{\sqrt{1-x}} + \frac{1}{(1-2x)^2/\sqrt{1-x} + 4x[(c_T/c_L)^2 - x]^{1/2}}\right]\right] .$$

Here ρ is the density of the metal and c_L and c_T are the longitudinal and transverse sound velocities. For most metals $c_T/c_L \approx \frac{1}{2}$ and for this case we show in Table I the contributions to $\xi_{\parallel}$ from emission of surface and bulk phonons. Obviously, almost the whole damping comes from emission of bulk phonons (more exactly, transverse bulk phonons with the displacement field parallel to the surface—see Appendix B). It is also of interest to know the damping of motion normal to the metal surface as it enters into various other dynamical processes. Again, it is shown in Appendix B that in this case (z is a coordinate normal to the surface)

$$F_{\perp} = -m\eta_{\perp}\dot{z}\ ,$$

where

$$\eta_{\perp} = \frac{1}{8\pi}\frac{m}{\rho}\left[\frac{\omega_0}{c_T}\right]^3 \xi_{\perp}\omega_0 \tag{37}$$

and

$$\xi_{\perp} = \mathrm{Re}\left[\int_0^{\infty} dx\, 2\left[\frac{(c_T/c_L)^2 - x}{1-x}\right]^{1/2} \frac{1}{(1-2x)^2/\sqrt{1-x} + 4x[(c_T/c_L)^2 - x]^{1/2}}\right] .$$

Table I shows that the dominating contribution to $\xi_{\perp}$ is emission of surface (Rayleigh) phonons. In Table II, we show $\eta_{\parallel}$ [as obtained from (36)] for a few different metals (in the calculation we have used $\omega_0 = 80\ \mathrm{cm}^{-1}$).

TABLE I. The contribution from emission of bulk and surface phonons, respectively, to the damping of modes parallel ($\xi_{\parallel}$) and normal ($\xi_{\perp}$) to the surface.

Friction parameter	Surface phonon	L + T bulk phonons	Total
$\xi_{\parallel}$	0.47	2.57	3.04
$\xi_{\perp}$	2.10	1.19	3.29

The formula given above for the friction force (sum over repeated indices)

$$F_{\alpha}(t) = -m\eta_{\alpha\beta}\dot{x}_{\beta}(t)\ , \tag{38}$$

TABLE II. Friction coefficient $\eta_{\parallel}$ for some metals using $\omega_0 = 80\ \mathrm{cm}^{-1}$ and $m=28$ u (CO). The friction coefficient for other resonance frequencies ω_0 and masses m can be obtained by scaling, using $\eta_{\parallel} \sim m\omega_0^4$.

Metal	Pt	Ni	Al	Cu
$\eta_{\parallel}$ (cm^{-1})	14.4	6.4	20.8	14.4

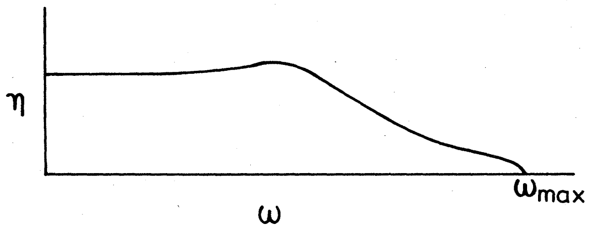

FIG. 1. General behavior of the friction parameter η as a function of frequency. $\omega_{\max}$ is the highest phonon frequency.

or with the time dependence Fourier transformed

$$F_\alpha(\omega)=i\omega m\eta_{\alpha\beta}x_\beta(\omega)\ ,$$

is valid within the elastic continuum model, i.e., for $\omega \ll \omega_{\max}$.

It is clear, however, that in general $\eta_{\alpha\beta}$ will depend on ω. For example, under the assumption that the coupling between the x motion and the crystal is harmonic, one must have $\eta_{\alpha\beta}(\omega)\rightarrow 0$ as $\omega\rightarrow\omega_{\max}$ since no damping can occur for $\omega>\omega_{\max}$. Thus one expects $\eta_{\alpha\beta}(\omega)$ to have the general form shown in Fig. 1. In reality, $\eta_{\alpha\beta}(\omega)$ is nonzero also for $\omega>\omega_{\max}$, since it is possible to couple to electron-hole pair excitations and also since the coupling to the crystal is never purely harmonic so that decay via multiphonon emission can occur. For the most general case, one writes

$$F_\alpha(t)=-m\int_0^t dt'\,\eta_{\alpha\beta}(t-t')\dot{x}_\beta(t')\ , \tag{39}$$

where the memory function $\eta_{\alpha\beta}(t)$ depends on the detailed molecule-crystal interaction. The derivation of the vibrational line shape in Sec. II A is only valid within the so-called Markoff approximation where (38) holds, i.e., when the memory function

$$\eta_{\alpha\beta}(t-t')=\eta_{\alpha\beta}\delta(t-t')$$

has no memory, making $\eta_{\alpha\beta}(\omega)$ frequency independent.

IV. EXPERIMENTAL RESULTS

In this work we present experimental data on the internal stretch vibrational mode of CO chemisorbed on a Ni(111) surface. The temperature dependence of the infrared absorption peak position and width has been studied. The experimental details of the infrared spectrometer have been given elsewhere.[8,24] The Ni crystal was oriented within $\frac{1}{2}$° mechanically and electropolished, and then cleaned by repeated cycles of heating to 1100 K, 200 L O_2 exposures at 300 K and argon ion sputtering. [1 L (langmuir)$\equiv 10^{-6}$ Torr sec.] The adsorption stages of CO/Ni(111) followed in general the work of Erley *et al.*[25] At sufficiently low temperatures first an ordered $c(4\times 2)$ structure with a basis of two molecules giving a coverage of 0.5 (with respect to the surface Ni atoms) was found, with all molecules in bridge position. Higher exposures gave a $(\sqrt{7}/2\times\sqrt{7}/2)R\,19^\circ$ structure (coverage 0.57) with every fourth molecule in the on-top position and the other bridge bonded. In Fig. 2 we present peak position and width as functions of temperature for the bridge-bonded molecules in the $c(4\times 2)$ structure and the terminal bonded molecules of the $(\sqrt{7}/2\times\sqrt{7}/2)R\,19^\circ$ structure. The widths were determined by integrating the first derivative spectra, taken with a modulation amplitude less than $\frac{1}{10}$ slit width. A typical derivative spectrum is also shown (after signal averaging for 5 min and subtracting of the measured background). The spectrometer resolution was 3 cm^{-1}, which has been subtracted from the data.

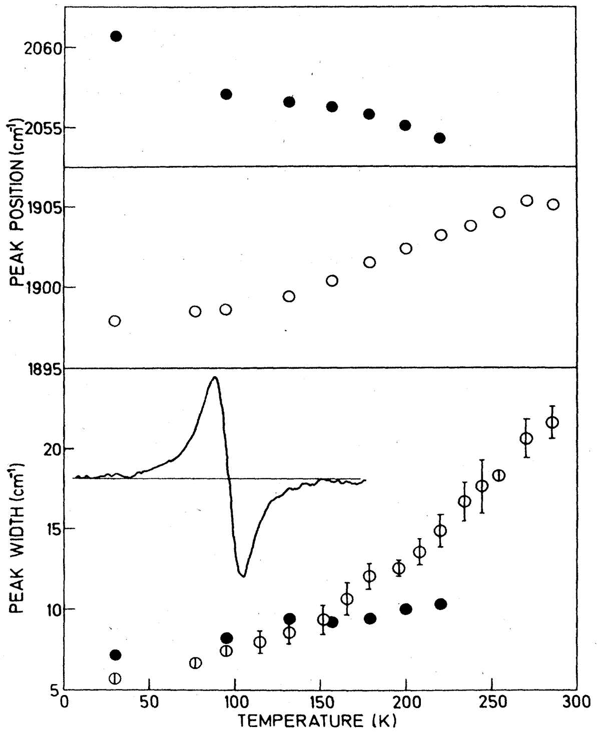

FIG. 2. Infrared absorption peak position and width (FWHM) as function of temperature for the internal stretch vibrational mode of CO on Ni(111). Bridge-bonded (○) and terminal bonded (●) molecules. Inserted is a typical first-derivative spectrum with a resolution of 3 cm^{-1}, an averaging time of 5 min, and with the background subtracted.

For the bridge-bonded molecules, which were of primary interest in this work, the widths were very sensitive to additional inhomogeneous broadening. This was probably caused by imperfections in the $c(4\times 2)$ structure (the on-top position is occupied for coverages both below[25] and above 0.5) that can be due to uncertainties in the exposure, readsorption during the heating of the sample, or minor surface contamination. For poorly-ordered structures we easily obtained an additional inhomogeneous broadening in the order of 10 cm^{-1}. In Fig. 2 we therefore present the mean value for four different depositions at each temperature and with a standard deviation of these four points as an error bar. The $c(4\times 2)$ structure is stable, as seen from the LEED pattern, below 300 K. The peak position, which was recorded by second-derivative spectra, was much more reproducible.

For the terminal-bonded molecules the situation is different. Most of the strength of their absorption peak is

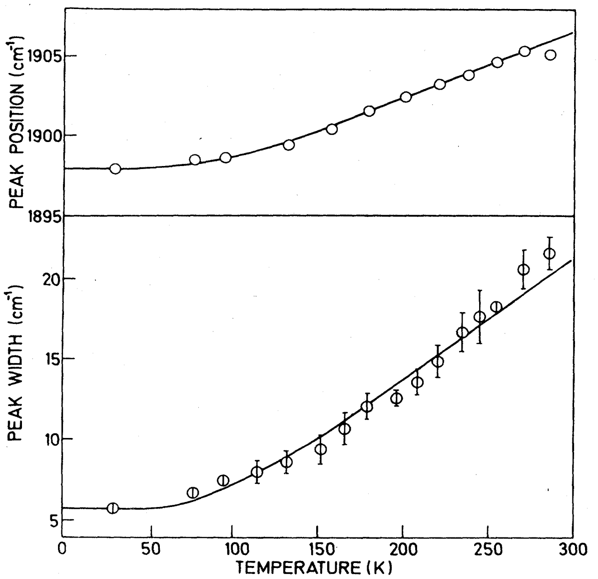

FIG. 3. Peak position and width for bridge-bonded molecules (○) reproduced from Fig. 2. The solid lines are the theoretical calculations using $\omega_0=220$ cm^{-1}, $\eta=37.5$ cm^{-1}, and $\delta\omega=34.4$ cm^{-1}.

caused by intensity transfer from the bridge-bonded molecules due to the dipole-dipole interaction.[26] Consequently, changes in the width and position of the bridge-bonded molecules will also influence this high-frequency peak. The $(\sqrt{7}/2\times\sqrt{7}/2)R\,19°$ structure was only stable below 230 K.

Except for the temperature-dependent features that will be discussed in the next section, it is interesting to note that the temperature independent part of the width for the bridge-bonded molecules is much smaller than what has previously been reported on transition metals. The low-temperature value places an upper bound to the vibrational damping rate, which then turns out to be at most only 30% larger than on Cu. Again, the value for the on-top molecules is not a good measure of the intrinsic linewidth due to the strong dipole-dipole coupling.

Although our results show the same general temperature dependence of the width as the previously reported study on the same system by Trenary *et al.*,[12] there exist some important discrepancies. For the $c(4\times2)$ structure we find an upward frequency shift of 8 cm^{-1} compared to a negligible (or a possible 6 cm^{-1} downward) shift with increasing temperature. Furthermore, the absolute values of the widths that we obtain is about half of that of Trenary *et al.* Part of the reason for these differences is probably due to our better sensitivity and resolution. In addition, the adsorbate structures were created using different procedures. We found that the sequence that gave the best ordered structure was to adsorb 3.0 L CO at 100 K, followed by a short anneal at 230 K. The structure was checked during each measurement by low-energy electron diffraction (LEED) and the $I(V)$ curve of the (0,0) beam. As mentioned above, the width was very sensitive to inhomogeneities in the structure, which forced us to make an average of four values at each temperature.

V. ANALYSIS OF EXPERIMENTAL DATA

In this section, we will analyze the experimental data using the theory discussed above. Figure 3 shows the peak width (FWHM) and center frequency for the internal stretch vibration for CO in bridge position on Ni(111). The open circles are experimental data and the solid lines are calculated from Eqs. (29)—(34). In the calculation we have used $\omega_0=220$ cm^{-1}, $\eta=37.5$ cm^{-1}, and $\delta\omega=34.4$ cm^{-1}. The overall agreement between theory and experiment is very good. For low enough temperatures, the low-frequency mode ω_0 is frozen out so that $\Delta\omega$ and γ becomes almost temperature independent for $k_B T \ll \hbar\omega_0$.

Let us now discuss the implications of the values of the parameters ω_0, η, and $\delta\omega$ found above. Richardson and Bradshaw[27] have performed a normal mode analysis of CO bonded in the bridge position on a small nickel cluster. Of all the normal modes involving CO, only the frustrated translation ω_{tra} and the frustrated rotation ω_{rot} (see Fig. 4) have resonance energies below the maximum Ni phonon frequency ($\simeq 290$ cm^{-1}). The next-lowest vibrational mode is the metal-CO stretch vibration at the frequency $\omega_0 \approx 360$ cm^{-1}. This mode has probably a width (FWHM) of the order of 15 cm^{-1}, damped via two-phonon emission. The calculated frequencies for the frustrated translation and rotation should only be taken as very rough estimates. It is nevertheless satisfying to find

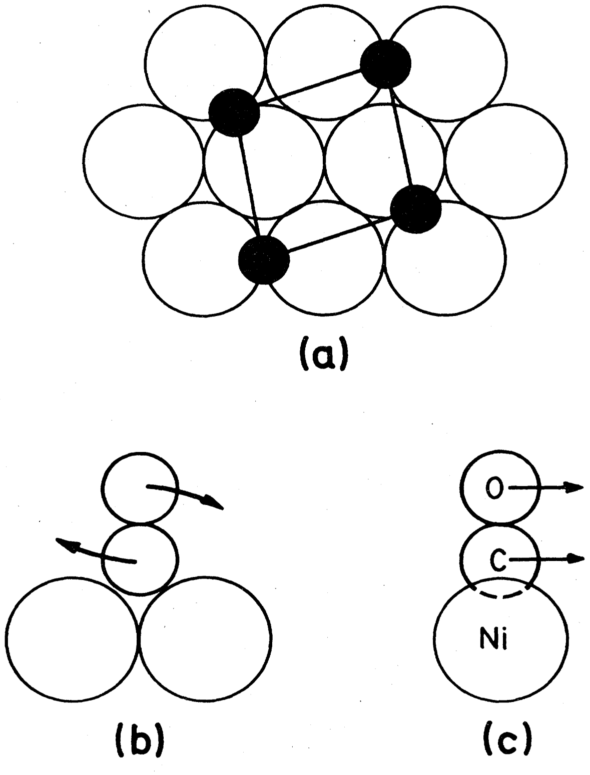

FIG. 4. (a) Position of the bridge-bonded CO molecules in the $c(4\times2)$ structure on Ni(111). (b) Schematic picture of the frustrated rotation, $\omega_{\mathrm{rot}}\approx 184$ cm^{-1}. (c) The frustrated translation, $\omega_{\mathrm{tra}}\approx 76$ cm^{-1}.

that the frequency $\omega_0 = 220\ \text{cm}^{-1}$, that we have obtained by comparing theory with experiment, is close to the calculated $\omega_{\text{rot}} = 184\ \text{cm}^{-1}$ while it is a factor of 3 larger than $\omega_{\text{tra}} = 76\ \text{cm}^{-1}$. Thus we argue that *the vibrational phase relaxation* in the present case *involves coupling to the frustrated rotation* ω_{rot}.

Next, let us discuss the magnitude of the friction coefficient $\eta = 38\ \text{cm}^{-1}$. We can estimate η theoretically using the theory presented in Sec. IV and Appendix B. First we note that $\omega_0 = 220\ \text{cm}^{-1}$ is so large compared with the highest bulk phonon frequency $\omega_{\max} = 290\ \text{cm}^{-1}$ that we cannot directly use the continuum model result. However, based on the known (for $\omega \ll \omega_{\max}$) relative magnitudes between emission of transverse and longitudinal bulk phonons and surface (Rayleigh) phonons, we have shown in Fig. 1 the approximate frequency dependence of $\xi_{\parallel}$ and $\xi_{\perp}$ and using this figure and Eqs. (36) and (37) we get $\xi_{\parallel} \approx \xi_{\perp} \approx 0.5$ and $\eta_{\parallel} \approx \eta_{\perp} \approx 45\ \text{cm}^{-1}$, which is consistent with the obtained $\eta = 38\ \text{cm}^{-1}$. We have also estimated η for a pure rotation and find $\eta_{\text{rot}} \approx 40\ \text{cm}^{-1}$.

It is not possible to estimate $\delta\omega$ theoretically without an extensive chemisorption calculation, which is not yet available. However, we would like to make one qualitative point. In Fig. 5(a) we show the lowest unoccupied molecular orbital ($2\pi^*$) and the highest occupied molecular orbital (5σ), which are the orbitals that are expected to be most involved in the chemisorption. The 5σ is essentially nonbonding, with respect to the C-O separation, and we expect that changes in the 5σ-metal bond as the CO molecule is tilted will have little influence on the C—O stretch frequency. On the other hand, the $2\pi^*$ molecular orbital (MO's) are antibonding with respect to the C-O separation. For chemisorbed CO, the $2\pi^*$ level forms a partly-filled resonance located in the vicinity of the Fermi energy. In the bridge position, there is an appreciable overlap between the $2\pi^*$ and the metal orbitals [see Fig. 5(a)] leading to a relatively large charge transfer into the $2\pi^*$ level and consequently a lowering of the C—O stretch frequency when going from the on-top to bridge position. As the CO molecule is tilted, this overlap will change appreciably, leading to a relatively large change in the vibration frequency, i.e., $|\partial\Omega/\partial\Theta| \sim \delta\omega$ is large.

For CO on the *on-top* position, on the other hand, the $2\pi^*$ MO's are less involved [Fig. 5(b)] making $\delta\omega$ smaller. Furthermore, the frustrated rotation has stiffened[27] to $\omega_{\text{rot}} = 411\ \text{cm}^{-1}$ which is well above the highest phonon frequency of Ni. Thus we expect the damping, η_{rot}, to be considerably smaller than that for CO in bridge position. The small magnitude of $\delta\omega$ and η and the large magnitude of ω_{rot} (corresponding to a temperature of about $\simeq 600$ K) explain why the phase relaxation is so much weaker in the on-top position. Based on estimates of $\delta\omega$ and η for the low-frequency frustrated translations one can also understand why these modes give in general a negligible contribution to the phase relaxation process.

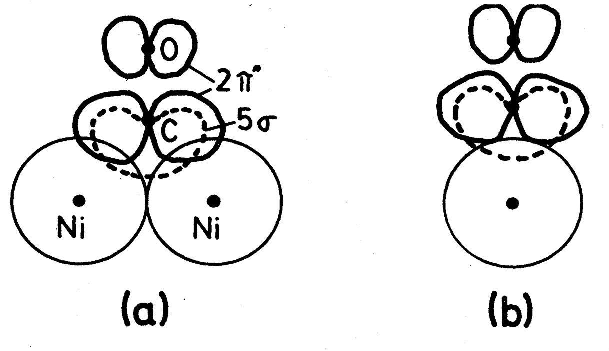

FIG. 5. The 5σ and $2\pi^*$ MO's of CO. (a) Bridge position. (b) On-top position

Finally, let us present a short discussion of the experimental data by Trenary *et al.* Since they observe negligible frequency shift compared with the increase in linewidth, the condition $\delta\omega \gg \eta$ must be satisfied. Thus at low temperatures ($k_B T \ll \hbar\omega_0$) one has [see (27) and (28)]

$$\gamma \approx 2\eta e^{-\beta\omega_0},$$

$$\Delta\omega \approx (\eta^2/\delta\omega) e^{-\beta\omega_0}.$$

The best fit of the linewidth is obtained with $\omega_0 \approx 700\ \text{cm}^{-1}$. At room temperature ($k_B T \approx 200\ \text{cm}^{-1}$), $\gamma \approx 30\ \text{cm}^{-1}$ so that

$$\eta \approx \gamma e^{\beta\omega_0}/2 \approx 500\ \text{cm}^{-1}$$

and

$$|\delta\omega| \approx |\eta^2/\Delta\omega|\, e^{-\beta\omega_0} \gtrsim 1000\ \text{cm}^{-1}$$

since $|\Delta\omega| \lesssim 7\ \text{cm}^{-1}$. These values for η and $\delta\omega$ are unphysical. Since the frequency ω_0 is well above the highest phonon frequency of the metal, the damping η is expected to be rather small, $\eta \sim 10\ \text{cm}^{-1}$. The quantity $\delta\omega$ is the frequency shift of the C—O stretch mode as the low-frequency mode ω_0 is in its first excited state. This frequency shift can hardly be as large as $|\delta\omega| \gtrsim 1000\ \text{cm}^{-1}$.

VI. OTHER PHASE RELAXATION PROCESSES

The vibrational-phase relaxation process discussed above is, of course, not the only possible one. For example, the C—O stretch vibration is coupled *directly* to the metal substrate via the anharmonic metal-CO binding potential and this coupling gives a contribution to the vibrational phase relaxation process as has been discussed in detail elsewhere.[15]

The temperature dependence of this contribution to the linewidth is $\gamma \sim T^2$ as $T \to \infty$ and $\gamma \sim T^3$ as $T \to 0$. Thus it does not exhibit an exponential low-temperature dependence as for the exchange coupling. For the system CO-Ni(111) one can estimate that the contribution to the room-temperature linewidth of the C—O stretch from the direct molecule-metal coupling is $\sim 0.1\ \text{cm}^{-1}$, i.e., an entirely negligible contribution.

The lateral interaction between adsorbed CO molecules will also give a contribution to the vibrational linewidth. This process is similar to the collisional broadening occurring in a gas of molecules. For an ordered system of adsorbed CO molecules, one must, in general, account both for the long-range dipole-dipole interaction as well as for the short-range (usually repulsive) interaction caused by the direct contact between two nearby molecules. It is easy to show that the dipole-dipole interaction gives a negligible contribution to the linewidth, but the contribution to the linewidth from the short-range interaction is more difficult to estimate since much less is known about its nature.

VII. SUMMARY AND CONCLUSION

In this work we have presented experimental results for the temperature dependence of the C—O stretch vibrational line for CO on Ni(111). These data have been analyzed within a simple theoretical model and remarkably good agreement between theory and experiment was obtained. We found that the temperature-dependent contribution to the C—O stretch vibrational line shape for CO in the twofold bridge position on Ni(111) involves coupling to a frustrated rotation with frequency $\omega_{\rm rot}\simeq 220$ cm^{-1} and damping (via one-phonon emission) $\eta\simeq 38$ cm^{-1}. We have presented theoretical results for the high-temperature dependence of the vibrational line shape thus extending the low-temperature results by Harris *et al.*[22] We have also shown that the relative importance of energy and phase relaxation for a chemisorbed molecule critically depends on its normal mode spectrum, the absorption site, and the properties of the substrate.

ACKNOWLEDGMENTS

We would like to thank A. Sjölander for useful discussions and M. Persson for critical comments on the manuscript.

APPENDIX A

Consider a diatomic molecule *AB* adsorbed on a metal surface. Let Ω be the frequency of the *A*—*B* stretch. It is assumed that Ω is much larger than any other vibration frequency of the system. Ω depends on the coordinates of a small number of nearby lattice atoms. We call these atoms together with the *A* and *B* atoms for the cluster. If the cluster were isolated (i.e., not interacting with the rest of the crystal) then the equation of motion for the cluster atoms would be

$$\ddot{\mathbf{x}}+\overleftrightarrow{\omega}^2\cdot\mathbf{x}=F(\mathbf{x}) \ , \tag{A1}$$

where $\overleftrightarrow{\omega}$ is the frequency matrix which, within the harmonic approximation, determines the normal mode frequencies of the cluster, and where $F(\mathbf{x})$ is an anharmonic coupling between the *AB* molecule and the rest of the cluster. Now, if the metal crystal is harmonic, then it is possible to account (exactly) for the coupling between the cluster and the rest of the crystal by simply replacing (A1) with[17–19]

$$\ddot{\mathbf{x}}+\overleftrightarrow{\omega}^2_{\rm eff}\cdot\mathbf{x}+\int_0^t dt'\,\overleftrightarrow{\eta}(t-t')\cdot\dot{\mathbf{x}}(t') + \overleftrightarrow{\eta}(t)\cdot\mathbf{x}(0)=\mathbf{f}(t)+\mathbf{F}(\mathbf{x}) \ . \tag{A2}$$

This equation differs from (A1) in three ways. Firstly, the frequency matrix $\overleftrightarrow{\omega}\rightarrow\overleftrightarrow{\omega}_{\rm eff}$, i.e., the cluster frequencies are renormalized due to the interaction between the cluster and the rest of the crystal. Secondly, a friction force has been introduced which describes the energy flow from the cluster to the rest of the crystal. Finally, a fluctuating force $\mathbf{f}(t)$ is introduced which, in accordance to the fluctuation-dissipation theorem must satisfy

$$\langle \mathbf{f}(t)\mathbf{f}(0)\rangle = k_B T\,\overleftrightarrow{\eta}(t) \ .$$

It is convenient to introduce normal mode coordinates and write

$$\mathbf{x}=\sum_\mu Q_\mu \mathbf{e}_\mu \ ,$$

where

$$\mathbf{e}_\mu\cdot\mathbf{e}_\nu=\delta_{\mu\nu}$$

and

$$\overleftrightarrow{\omega}_{\rm eff}\cdot\mathbf{e}_\mu=\omega_\mu\mathbf{e}_\mu \ .$$

Equation (A2) now reduces to

$$\ddot{Q}_\mu+\omega_\mu^2 Q_\mu+\int_0^t dt'\sum_\nu \eta_{\mu\nu}(t-t')\dot{Q}_\nu(t')+\sum_\nu \eta_{\mu\nu}(t)Q_\nu(0) = f_\mu(t)+F_\mu(Q_\nu) \ ,$$

where

$$\langle f_\mu(t)f_\nu(0)\rangle = k_B T \eta_{\mu\nu}(t)$$

and

$$F_\mu=\mathbf{e}_\mu\cdot\mathbf{F} \ .$$

We now assume that

$$\eta_{\mu\nu}(t)=2\eta_\mu\delta_{\mu\nu}\delta(t) \ .$$

We then get

$$\ddot{Q}_\mu+\omega_\mu^2 Q_\mu+\eta_\mu\dot{Q}_\mu=f_\mu(t)+F_\mu(Q_\nu) \ . \tag{A3}$$

Assume that the *A*—*B* stretch mode couples mainly to one low-frequency frustrated translation or rotation of the *AB* molecule. Let Q and ω_0 denote the corresponding normal mode coordinate and frequency. We get

$$\Omega^2=\Omega^2(Q)\approx\Omega_0^2+a\Omega_0 Q^2 \ ,$$

where we have expanded $\Omega^2(Q)$ to second order in Q and assumed that the linear term vanishes because of symmetry. Thus, if $u(t)$ denotes the normal mode coordinate of the *A*—*B* stretch, then it satisfies

$$m^*\ddot{u}+m^*(\Omega_0^2+a\Omega_0 Q^2)u=0 \ .$$

Here we have assumed that the *A*—*B* stretch vibration is undamped. In reality, this motion is damped due to excitation of electron-hole pairs but this just adds a temperature-independent contribution to the infrared (IR) linewidth (see Secs. IV and V). The low-frequency mode Q satisfies an equation of the type (A3)

$$\ddot{Q}+\omega_0^2 Q+\eta\dot{Q}=f(t)/m-a\Omega_0(m^*/m)u^2 Q \ ,$$

where

$$\langle f(t)f(0)\rangle = 2\eta m k_B T\delta(t) \ ,$$

where m is an effective mass.

APPENDIX B

Here we will derive (within the elastic continuum model) the friction parameters $\eta_{\parallel}$ and $\eta_{\perp}$ for the motion parallel and perpendicular to the surface, respectively.

We consider first the following general problem: On the surface of a semi-infinite medium acts a surface tension ($z=0$),

$$\sigma_{j3}=a_j^0 e^{i(\mathbf{k}_{\parallel}\cdot\mathbf{x}_{\parallel}-\omega t)}\equiv a_j(\mathbf{x}_{\parallel},t) . \tag{B1}$$

We want to calculate the resulting displacement field $u_j(\mathbf{x},t)$. This is a standard problem in mathematical physics and is most easily solved by decomposing the displacement field as

$$\mathbf{u}=\mathbf{p}A+\mathbf{K}B+\mathbf{p}\times\mathbf{K}C . \tag{B2}$$

Here A, B, and C are three scalar fields and $\mathbf{p}=-i\nabla, \mathbf{K}=-i\hat{\mathbf{z}}\times\nabla$. Substituting (B2) into the equation of motion

$$\sigma_{ij,j}=\rho\frac{\partial^2 u_i}{\partial t^2} ,$$

results in three scalar equations

$$\left[\frac{\partial^2}{\partial t^2}-c_{\mathrm{L}}^2\nabla^2\right]A=0 , \tag{B3}$$

$$\left[\frac{\partial^2}{\partial t^2}-c_{\mathrm{T}}^2\nabla^2\right]\begin{bmatrix}B\\C\end{bmatrix}=0 . \tag{B4}$$

It is obvious from (B2) that A is associated with the longitudinal displacement field and B and C with the two transverse displacement fields. Note also that $\mathbf{K}B$ is parallel to the metal surface.

We write

$$\sigma_{ij}=(a-b)u_{k,k}\delta_{ij}+b(u_{i,j}+u_{j,i}) , \tag{B5}$$

where

$$c_{\mathrm{T}}^2=b/\rho,\quad c_{\mathrm{L}}^2=(a+b)/\rho .$$

Substituting (B2) and (B5) in (B1) gives

$$\hat{\mathbf{z}}(a-b)p^2A+\mathbf{p}b(2p_zA+K^2C)$$
$$+\mathbf{K}bp_zB+\mathbf{p}\times\mathbf{K}bp_zC=-i\mathbf{a} .$$

From this equation one obtains three scalar equations by operating with $\mathbf{n}\cdot$, $\mathbf{K}\cdot$, and $\mathbf{p}_{\parallel}\cdot$:

$$\begin{aligned}&[(a-b)p^2+(a+b)p_z^2]A+2bp^2p_zC=-ia_z ,\\ &bp^2p_zB=i(k_ya_x-k_xa_y) ,\\ &bp^2[2p_zA+(p^2-p_z^2)C]=-i(k_xa_x+k_ya_y) .\end{aligned} \tag{B6}$$

The general solutions to (B3) and (B4) consistent with the boundary condition (B1) are

$$\begin{aligned}&A=A_0e^{i(\mathbf{k}_{\parallel}\cdot\mathbf{x}_{\parallel}+p_Lz-\omega t)} ,\\ &\begin{bmatrix}B\\C\end{bmatrix}=\begin{bmatrix}B_0\\C_0\end{bmatrix}e^{i(\mathbf{k}_{\parallel}\cdot\mathbf{x}_{\parallel}+p_Tz-\omega t)} ,\end{aligned} \tag{B7}$$

where

$$p_{\mathrm{L}}=\left[\frac{\omega^2}{c_{\mathrm{L}}^2}-k_{\parallel}^2\right]^{1/2} ,$$

$$p_{\mathrm{T}}=\left[\frac{\omega^2}{c_{\mathrm{T}}^2}-k_{\parallel}^2\right]^{1/2} .$$

Now we consider two cases.

Case 1. Assume $a_x=a_y=0$. Substituting (B7) in (B6) gives $B=0$ and

$$A_0=\frac{1}{2p_{\mathrm{L}}}(p_{\mathrm{T}}^2-k_{\parallel}^2)C_0 ,$$

$$C_0=-i\frac{a_z^0}{[(a-b)k_{\parallel}^2+(a+b)p_{\mathrm{L}}^2[(p_{\mathrm{L}}^2-k_{\parallel}^2)/2p_{\mathrm{L}}]+2bk_{\parallel}^2p_{\mathrm{T}}}$$
$$\equiv\frac{-ia_z^0}{Q} ,$$

from which one can calculate $u_3\,(0,t)$:

$$\begin{aligned}u_3&=p_zA+K^2C=\tfrac{1}{2}(k_{\parallel}^2+p_{\mathrm{T}}^2)C\\ &=\frac{-i(k_{\parallel}^2+p_{\mathrm{T}}^2)a_z}{2Q} .\end{aligned} \tag{B8}$$

Case 2. Assume $a_y=a_z=0$. Substituting (B7) in (B6) gives

$$B_0=i\frac{k_ya_x}{bk_{\parallel}^2p_{\mathrm{T}}} ,$$

$$C_0=\frac{-1}{2bk_{\parallel}^2p_{\mathrm{T}}}[(a-b)k_{\parallel}^2+(a+b)p_{\mathrm{L}}^2]A_0 ,$$

$$A_0=-ik_xa_x\frac{p_{\mathrm{T}}}{p_{\mathrm{L}}}\frac{1}{Q} ,$$

from which one can calculate $u_1(0,t)$:

$$\begin{aligned}u_1&=p_xA-p_yB-p_xp_yC\\ &=-ik_y^2\frac{a_x}{bk_{\parallel}^2p_{\mathrm{T}}}-ik_x^2\frac{\omega^2}{c_{\mathrm{T}}^2}\frac{a_x}{2k_{\parallel}^2}\frac{p_{\mathrm{T}}}{p_{\mathrm{L}}}\frac{1}{Q} .\end{aligned} \tag{B9}$$

Let us now return to the original problem, namely the calculation of the memory functions $\eta_{\parallel}(\omega)$ and $\eta_{\perp}(\omega)$. Let us first consider motion of the particle in the x direction:

$$m\ddot{x}+m\bar{\omega}_0^2[x-u_1(0,t)]=f(t) . \tag{B10}$$

The force on the elastic medium is $\sigma_{23}=\sigma_{33}=0$ and

$$\sigma_{13}=m\bar{\omega}_0^2[u_1(0,t)-x(t)]\delta(\mathbf{x})$$

or

$$\sigma_{13}=m\bar{\omega}_0^2[u_1(0,\omega)-x(\omega)]\frac{1}{(2\pi)^2}\int d^2k_{\parallel}\,e^{i(\mathbf{k}_{\parallel}\cdot\mathbf{x}_{\parallel}-\omega t)} .$$

Using (B9) we now get

$$u_1(0,\omega)=m\bar{\omega}_0^2[u_1(0,\omega)-x(\omega)]\frac{1}{(2\pi)^2}$$
$$\times\int d^2k\left[-i\frac{k_y^2}{bk_{\parallel}^2p_{\mathrm{T}}}-i\frac{\omega^2}{c_{\mathrm{T}}^2}\frac{k_x^2}{2k_{\parallel}^2}\frac{p_{\mathrm{T}}}{p_{\mathrm{L}}}\frac{1}{Q}\right]$$

or

$$u_1(0,\omega)=F(\omega)x(\omega)\ , \tag{B11}$$

where

$$F(\omega)=\frac{R(\omega)}{1+R(\omega)} \tag{B12}$$

with

$$\mathrm{Im}R(\omega)=\frac{1}{8\pi}\frac{m}{\rho}\left[\frac{\omega_0}{c_{\mathrm{T}}}\right]^3\xi_{\parallel}\frac{\omega}{\omega_0}\ ,$$

where $\xi_{\parallel}$ is given in Sec. III. We now write $R=R_0+iR_1$ where R_0 and R_1 are real. Now $R_1\sim\omega$ so that for small enough ω (see below) $|R_1|\ll 1$ and we can approximate

$$\frac{1}{1+R}\approx\frac{1}{1+R_0}-i\frac{R_1}{(1+R_0)^2}\ . \tag{B13}$$

Consider now the equation of motion (B10)

$$-\omega^2x(\omega)+\bar{\omega}_0^2[x(\omega)-u_1(0,\omega)]=f(\omega)/m\ ,$$

or with (B11) and (B12):

$$-\omega^2x(\omega)+\bar{\omega}_0^2\frac{1}{1+R}x(\omega)=f(\omega)/m\ .$$

Thus, using (B13),

$$-\omega^2x(\omega)+\frac{\bar{\omega}_0^2}{1+R_0}x(\omega)-i\frac{\bar{\omega}_0^2}{1+R_0}\frac{R_1}{1+R_0}x(\omega)=f(\omega)/m\ .$$

We write

$$\frac{\bar{\omega}_0^2}{1+R_0}=\omega_0^2\ ,$$

$$\frac{\bar{\omega}_0^2}{1+R_0}\frac{R_1}{1+R_0}=\frac{1}{8\pi}\frac{m}{\rho}\left[\frac{\omega_0}{c_{\mathrm{T}}}\right]^3\xi_{\parallel}\omega_0\omega\equiv\eta_{\parallel}\omega\ ,$$

so that

$$-\omega^2x(\omega)+\omega_0^2x(\omega)-i\omega\eta_{\parallel}x(\omega)=f(\omega)/m$$

or

$$\ddot{x}+\omega_0^2x+\eta_{\parallel}\dot{x}=f(t)/m\ .$$

Thus, the coupling to the substrate will renormalize the oscillator frequency $\bar{\omega}_0\rightarrow\omega_0$ and introduce a friction $\eta_{\parallel}$. In an analogous way, one can derive the expressions for $\eta_{\perp}$ given in Sec. III.

---

[1] A. Laubereau and W. Kaiser, in *Chemical and Biological Applications of Lasers,* edited by C. B. Moore (Academic, New York, 1977), Vol. II.

[2] S. Marks, P. A. Cornelius, and C. B. Harris, J. Chem. Phys. **73**, 3069 (1980).

[3] Ph. Avouris and B. N. J. Persson, J. Phys. Chem. **88**, 837 (1984).

[4] J. W. Gadzuk and A. C. Luntz, Surf. Sci. **144**, 429 (1984).

[5] B. N. J. Persson, J. Phys. C **11**, 4251 (1978); B. N. J. Persson and M. Persson, Solid State Commun. **36**, 609 (1980).

[6] A. Laubereau, Chem. Phys. Lett. **27**, 600 (1974).

[7] Y. J. Chabal and A. J. Sievers, Phys. Rev. Lett. **44**, 944 (1980).

[8] R. Ryberg, Surf. Sci. **113**, 627 (1982).

[9] F. M. Hoffman, Surf. Sci. Rep. **3**, 107 (1983).

[10] B. E. Hayden and A. M. Bradshaw, Surf. Sci. **125**, 787 (1983).

[11] S. Chiang, R. G. Tobin, P. L. Richards, and P. A. Thiel, Phys. Rev. Lett. **52**, 648 (1984).

[12] M. Trenary, K. J. Vram, F. Bozso, and J. T. Yates, Jr., Surf. Sci. **146**, 269 (1984).

[13] R. Ryberg (unpublished).

[14] J. C. Ariyasu, D. L. Mills, K. G. Lloyd, and J. C. Hemminger, Phys. Rev. B **28**, 6123 (1983).

[15] B. N. J. Persson, J. Phys. C **17**, 4741 (1984).

[16] B. N. J. Persson and E. Zaremba, Phys. Rev. B **31**, 1863 (1985).

[17] R. W. Zwanzig, J. Chem. Phys. **32**, 1173 (1960).

[18] S. A. Adelman and J. D. Doll, J. Chem. Phys. **61**, 4242 (1974); **64**, 2375 (1976).

[19] M. Shugard, J. C. Tully, and A. Nitzan, J. Chem. Phys. **66**, 2534 (1977); A. Nitzan, M. Shugard, and J. C. Tully, *ibid.* **69**, 2525 (1978); J. C. Tully, *ibid.* **73**, 1975 (1980).

[20] B. N. J. Persson (unpublished).

[21] R. Kubo, J. Phys. Soc. Jpn. **17**, 1100 (1962).

[22] C. B. Harris, R. M. Shelby, and P. A. Cornelius, Phys. Rev. Lett. **38**, 1415 (1977); R. M. Shelby, C. B. Harris, and P. A. Cornelius, J. Chem. Phys. **70**, 34 (1979).

[23] P. W. Anderson, J. Phys. Soc. Jpn. **9**, 316 (1954).

[24] R. Ryberg, J. Phys. (Paris) Colloq. **44**, C10-421 (1983).

[25] W. Erley, H. Wagner, and H. Ibach, Surf. Sci. **80**, 612 (1979).

[26] B. N. J. Persson and R. Ryberg, Phys. Rev. B **24**, 6954 (1981).

[27] N. V. Richardson and A. M. Bradshaw, Surf. Sci. **88**, 255 (1979).